A deep field weakening control for the PMSM applying a modified overmodulation strategy

Qian Liu, **Kay Hameyer****

* *Institute of Electrical Machines, RWTH Aachen University, Germany*
Email: qian.liu@iem.rwth-aachen.de

Keywords: Field weakening, overmodulation, robustness, PMSM.

Abstract

A field weakening control applying a modified overmodulation strategy is proposed to improve the stability of the PMSM drive system. The modified overmodulation is combined with the voltage feedback control to achieve a robust deep field weakening range for the machine. With the proposed control strategy, no switching is required between the MTPA, constant power and MTPV operating regions so that a seamless operation of the PMSM can be achieved. The proposed overmodulation guarantees that the current of the PMSM stays around its limitation during the transient state in the field weakening region. With an additional compensation term, a simple and stable control of MTPV operation for the PMSM can be achieved. In the end, the proposed control scheme is validated by simulation and experimental results.

1 Introduction

Nowadays, the PMSM is widely used in industry due to its high power density, high efficiency and excellent controllability. In some applications such as electrical vehicles, the electrical machine is required to be operated in a wide speed range. Therefore, it is expected that the PMSM possesses a deep field weakening capability to reduce the requirement on the DC-link voltage as well as the power rating of the inverter. The existing field weakening control can be distinguished into three categories: feedforward control, feedback control and mixed approaches [1].

The feedforward approach obtains the reference current using the PMSM model, the voltage and current constraints and the MTPV condition. Due to the strong nonlinearity between the torque and the voltage constraint of the PMSM, it is difficult to obtain the accurately analytical solution of the current reference in the field weakening region. Several strategies are made such as linearized approximation [2], polynomial approximation [3] and the stored LUT dependent on rotor speed [4, 5]. The feedforward approach is very sensitive to the parameter variation of the PMSM, which results in low robustness of the PMSM drive system. To guarantee the stability over the entire speed range, the feedforward approach is usually conservatively designed so that the PMSM is not fully utilized [1].

The feedback approach is based on a closed loop control of the voltage error between the unmodulated voltage and the voltage limit of the inverter. Two typical strategies of the feedback voltage control can be found in the existing literatures: the d-axis current [6, 7] or the phase angle of the stator current [1]. In the voltage feedback loop, the controller parameters are less dependent of the machine parameter. Therefore, the feedback approach is insensitive to the parameter variation of the PMSM and the performance is robust. However, it is only effective for the constant power operation. To realize the MTPV operation, the MTPV trajectory based on machine parameters and speed should be imposed [8–10]. Especially for the IPMSM, a judgment and a switching between constant power and MTPV regions are required, which degrades the system stability as well as the transient performance. Therefore, it is difficult for the feedback approach to reach the deep field weakening region. In recent years, a single current and voltage control approach is proposed to realize the deep field weakening region [11, 12]. However, a switching is still needed and the stability of this approach in the entire field weakening region is not guaranteed.

The mixed approach is a combination of the feedforward and feedback approaches [13]. The feedback loop amend the current reference from the feedforward approach to against the parameter variation. On the other hand, the requirement on the feedback controller can be loosed since the PMSM system can be treated as a linearized small signal model when it is with the feedforward current reference.

In this paper, a voltage feedback control with modified overmodulation and a MTPV compensation term is proposed to achieve a robust seamless deep field weakening range control for the PMSM. A modified overmodulation strategy is introduced to guarantee the transient stability of the flux in the field weakening region. A penalty factor is utilized to modify the amplitude of the reference current to realize a smooth transition from constant power region to MTPV region of the PMSM. In the end, both simulation and experimental results validate the performance of the proposed field weakening control strategy.

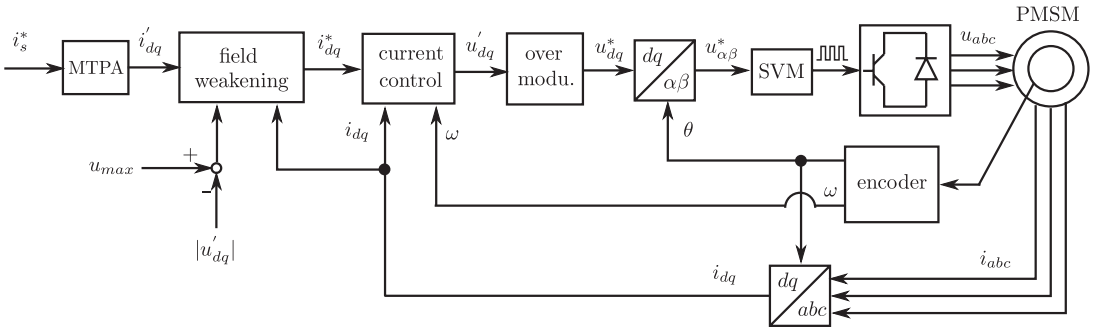

Fig. 1: General block diagram for the voltage feedback field weakening control.

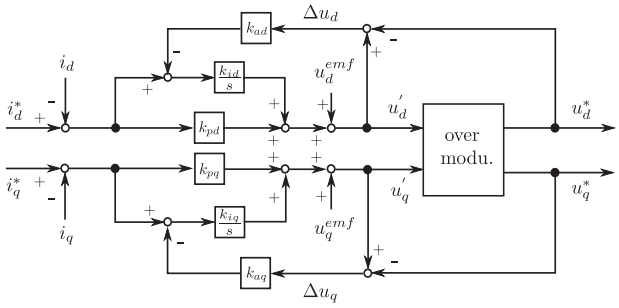

Fig. 2: Vector current control with anti-windup.

2 Model and basic control of the PMSM

The general block diagram of the current control of the PMSM with voltage feedback loop is shown in fig. 1. It consists of MTPA regulation, field weakening control with voltage feedback, current vector control and the overmodulation. The model of the PMSM in the dq coordinate system can be presented by the following equations:

$$\frac{di_d}{dt} = -\frac{R}{L_d}i_d + \frac{\omega L_q i_q}{L_d} + \frac{u_d}{L_d}, \tag{1}$$

$$\frac{di_q}{dt} = -\frac{R}{L_q}i_q - \frac{\omega L_d i_d}{L_q} - \frac{\omega \Psi_F}{L_q} + \frac{u_q}{L_q}, \tag{2}$$

where R, L_d, L_q and Ψ_F are the stator resistance, inductance on d,q-axis and the magnetic flux of the PMSM respectively. ω is the rotational speed in electrical radian.

The detailed principle of the vector control of the PMSM with anti wind-up is shown in fig. 2, where k_{pd}, k_{id}, k_{ad}, k_{pq}, k_{iq} and k_{aq} are the controller parameters. u_d^{emf} and u_q^{emf} are the back-emf voltages on d- and q-axis respectively:

$$u_d^{emf} = \omega\psi_q = -\omega L_q i_q, \tag{3}$$

$$u_q^{emf} = \omega\psi_d = \omega(L_d i_d + \psi_F). \tag{4}$$

With the anti-windup, the unmodulated voltage $u_d^{'}$ and $u_q^{'}$ can be expressed by the following equation [14]:

$$u_d^{'} = \frac{sk_{pd} + k_{id}}{s}(i_d^* - i_d) - \frac{k_{ad}k_{id}}{s}\Delta u_d, \tag{5}$$

$$u_q^{'} = \frac{sk_{pq} + k_{iq}}{s}(i_q^* - i_q) - \frac{k_{aq}k_{iq}}{s}\Delta u_q. \tag{6}$$

where

$$\Delta u_d = u_d^{'} - u_d^*, \qquad \Delta u_q = u_q^{'} - u_q^*. \tag{7}$$

For the conventional vector control, the closed loop of the current control is usually designed as decoupled low pass filters, when the voltage limit is not reached. The parameters of the current controller are chosen by:

$$k_{pd} = \frac{L_d}{\tau_i}, \qquad k_{id} = \frac{R}{\tau_i}, \qquad k_{ad}k_{id} = \frac{R}{L_d}, \tag{8}$$

$$k_{pq} = \frac{L_q}{\tau_i}, \qquad k_{iq} = \frac{R}{\tau_i}, \qquad k_{aq}k_{iq} = \frac{R}{L_q}, \tag{9}$$

where τ_i is a time constant determining the bandwidth of the current closed loop. Using equations (1) to (9) and the vector control with anti-windup, the current dynamics of the PMSM can be presented by the following equations:

$$i_d = \frac{1}{1+\tau_i s}i_d^* - \frac{\tau_i}{L_d}\frac{1}{1+\tau_i s}\Delta u_d, \tag{10}$$

$$i_q = \frac{1}{1+\tau_i s}i_q^* - \frac{\tau_i}{L_q}\frac{1}{1+\tau_i s}\Delta u_q. \tag{11}$$

3 Modified overmodulation strategy

When the output voltage of the current controller exceeds the maximum suppliable voltage of the inverter, it should be truncated by the voltage limitation so that it can be realized by the inverter. In the existing literature, three over modulation strategies are often utilized for the space vector modulation: the separated overmodulation [15], the minimum phase error overmodulation [16] and the dynamic overmodulation [17]. The current dynamics can be greatly influenced by the overmodulation strategy [17, 18]. The aforementioned overmodulation strategy are more concerned of the current dynamics

when compared to the system stability and robustness in the field weakening region.

In order to achieve a stable operation in the deep field weakening region, a modified overmodulation strategy is proposed in this section. Considering the stator fluxes ψ_d ψ_q of the PMSM and using the discrete model of the current dynamics (10) and (11), the discrete model of the flux dynamics can be presented by:

$$\psi_{d,k+1} = \psi_{d,k} + \frac{T_s}{\tau_i}(L_d i^*_{d,k} - L_d i_{d,k} - \tau_i \Delta u_{d,k}), \quad (12)$$

$$\psi_{q,k+1} = \psi_{q,k} + \frac{T_s}{\tau_i}(L_q i^*_{q,k} - L_q i_{q,k} - \tau_i \Delta u_{q,k}), \quad (13)$$

where T_s is the sampling time of the digital controller. The subscript k denotes the discrete time instant. The stator flux of the PMSM is calculated by $\psi_{s,k} = \sqrt{\psi^2_{d,k} + \psi^2_{q,k}}$. Using the small signal analysis, the differentiation of the stator flux of the PMSM can be evaluated by:

$$\Delta_k = \frac{1}{2}\frac{d\psi^2_{s,k}}{dt} \approx \psi_{d,k}\frac{\psi_{d,k+1} - \psi_{d,k}}{T_s} + \psi_{q,k}\frac{\psi_{q,k+1} - \psi_{q,k}}{T_s} \quad (14)$$

In the field weakening region, it is expected that Δu_d and Δu_q reduce the stator flux of the PMSM to fulfill the voltage constraint of the inverter. In another word, the following inequality is expected for a transiently stable overmodulation in the field weakening region:

$$\frac{\partial \Delta_k}{\partial \Delta \boldsymbol{u}_{dq,k}} \Delta \boldsymbol{u}_{dq,k} \leq 0 \quad (15)$$

where $\Delta \boldsymbol{u}_{dq,k} = [\Delta u_{d,k}, \Delta u_{q,k}]^T$ denotes the vector of the voltage difference. Using equations (12) to (14), the partial derivative of Δ_k can be expressed by the following equation:

$$\frac{\partial \Delta_k}{\partial \Delta \boldsymbol{u}_{dq,k}} \Delta \boldsymbol{u}_{dq,k} = -\psi_{d,k}\Delta u_d - \psi_{q,k}\Delta u_q \quad (16)$$

From equation (16), it can be noticed that if the vector $[\Delta u_{d,k}, \Delta u_{q,k}]^T$ is chosen to the same direction as the flux vector $[\psi_{d,k}, \psi_{q,k}]^T$, the inequality (15) holds. However, the calculation of $[\Delta u_{d,k}, \Delta u_{q,k}]^T$ is complicated. On the other hand, the estimation of the flux vector depends on the machine parameters, which degrades the robustness of the overmodulation. Therefore, a simplified strategy is introduced to overcome these drawbacks.

In the proposed overmodulation, the sign of the voltage $\boldsymbol{u}^*_{dq}$ is identical to the one of $\boldsymbol{u}^{'}_{dq}$, as well as the one of $\Delta \boldsymbol{u}_{dq}$. Therefore, it fulfills

$$\text{sign}(\Delta u_{d,k}) = \text{sign}(u^*_{d,k}) = \text{sign}(u^{'}_{d,k}), \quad (17)$$

$$\text{sign}(\Delta u_{q,k}) = \text{sign}(u^*_{q,k}) = \text{sign}(u^{'}_{q,k}). \quad (18)$$

On the other hand, the rotor speed of the PMSM is very high in the field weakening region. The back-emf voltage is the major component of the terminal voltage of the PMSM. Therefore, the sign of the voltage $\boldsymbol{u}_{dq}$ and $[u^{emf}_d, u^{emf}_q]^T$ can be considered identical. Neglecting the voltage distortion in the inverter, it holds:

$$u^*_{d,k} = u_{d,k} = -k_1 \omega \psi_{q,k}, \quad (19)$$

$$u^*_{q,k} = u_{q,k} = k_2 \omega \psi_{d,k}, \quad (20)$$

where k_1 and k_2 are positive real variables. Using equations (17) to (20), we have

$$\psi_{d,k}\Delta u_{d,k} = \frac{u^*_{q,k}\Delta u_{d,k}}{k_2\omega} = \frac{u^*_{q,k}|\Delta u_{d,k}|\text{sign}(-k_1\omega L_q i_{q,k})}{k_2\omega} = -\frac{L_q|u^*_{q,k}\Delta u_{d,k}|}{k_2|\omega|}\text{sign}(u^*_{q,k} i_{q,k}) \quad (21)$$

Similarly, the following equation for the q-axis also holds:

$$\psi_{q,k}\Delta u_{q,k} = L_q|i_{q,k}\Delta u_{q,k}|\text{sign}(u^*_{q,k} i_{q,k}) \quad (22)$$

With equations (18), (21) and (21), equation (16) can be reformed into the following form:

$$\frac{\partial \Delta_k}{\partial \Delta \boldsymbol{u}_{dq,k}} \Delta \boldsymbol{u}_{dq,k} = (\frac{|u^{'}_{q,k}\Delta u_{d,k}|}{k_2|\omega|} - |i_{q,k}\Delta u_{q,k}|) * L_q \text{sign}(u^{'}_{q,k} i_{q,k}). \quad (23)$$

Therefore, the overmodulation strategy can be chosen as:

$$\begin{cases} \Delta u_{d,k} = 0 & \text{if sign}(u^{'}_{q,k} i_{q,k}) > 0 \\ \Delta u_{q,k} = 0 & \text{otherwise} \end{cases} \quad (24)$$

With (24), it can be noticed that condition (15) can always be fulfilled. The decreasing stator flux guarantees the transient stability of the PMSM in the field weakening region. Reforming equation (24), the complete expression for the proposed overmodulation strategy can be presented by the following equations:

$$u^*_{d,k} = \begin{cases} u^{'}_{d,k} & \text{if sign}(u^{'}_{q,k} i_{q,k}) > 0 \\ \text{sign}(u^{'}_{d,k})\sqrt{u^2_{max} - u^{*2}_{q,k}} & \text{otherwise} \end{cases} \quad (25)$$

$$u^*_{q,k} = \begin{cases} \text{sign}(u^{'}_{q,k})\sqrt{u^2_{max} - u^{*2}_{d,k}} & \text{if sign}(u^{'}_{q,k} i_{q,k}) > 0 \\ u^{'}_{q,k} & \text{otherwise} \end{cases} \quad (26)$$

where u_{max} denotes the voltage constraint of the inverter. For the proposed overmodulation strategy, both circle and hexagon constraints can be applied. Furthermore, the proposed strategy is invariant with the back-emf voltage as well as the machine parameters. Therefore, the robustness of the proposed overmodulation against the parameter variation is relatively high when compared to the dynamic overmodulation strategy.

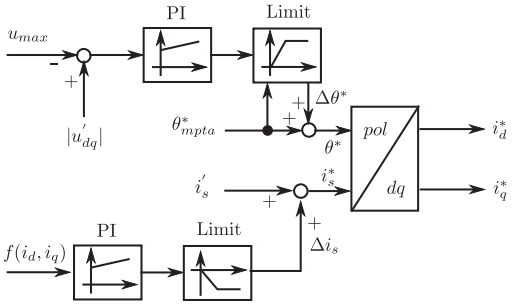

Fig. 3: Field weakening control with voltage feedback and current penalty.

4 Voltage feedback with current penalty

The proposed field weakening control with voltage feedback is shown in fig. 3, which is based on the modification of the amplitude and phase angle of the stator current reference i'_s. The reference angle θ_{mtpa} denotes the optimum phase angle of the Maximum Torque per Ampere (MTPA) condition corresponding to current amplitude i'_s. A field weakening angle $\Delta\theta$ is obtained by the standard PI voltage feedback loop.

In order to realize a deep field weakening control as well as a smooth transition between the constant power and the MTPV regions, a penalty term $f(i_d, i_q)$ is introduced to modify the amplitude of the current reference. The expression of $f(i_d, i_q)$ is described by:

$$\begin{aligned} f(i_d, i_q) =& L_d(\frac{L_d}{L_q} - 1)i_d^2 + \psi_F(\frac{2L_d}{L_q} - 1)i_d \\ &+ L_q(\frac{L_q}{L_d} - 1)i_q^2 + \frac{\psi_F^2}{L_q} \end{aligned} \tag{27}$$

In the current locus of the PMSM, $f(i_d, i_q) = 0$ denotes the MTPV operating curve and $f(i_d, i_q) < 0$ presents the area on the left side of the MTPA curve [19]. On the other hand, the current locus of the PMSM should stay on the right side of the MTPV curve to realize the maximum torque. Therefore, a PI feedback loop of $f(i_d, i_q)$ is introduced to penalize the amplitude of the current reference i'_s, when the current locus reaches the left side of the MTPV curve. The current compensation Δi_s is limited within the interval $(-\infty, 0]$.

The feedback loops of the voltage and the penalty term modify the phase angle and the amplitude of the current reference independently. Therefore, the corresponding phase angle and amplitude of the current reference on the MTPV curve can be achieved and stabilized by the cooperation of both feedback loops. Furthermore, no switching between the constant power and MTPV operation is needed so that a smooth transition in the field weakening region can be achieved. From equation (27), it can be noticed that the penalty term depends on the machine parameters. With parameter mismatch of the PMSM, the utilized MTPV curve will deviate from the real MTPV curve. However, the deviated MTPV curve does not influence the stability of the field weakening control. The PMSM will be stabilized at the operating point with corresponding load on the deviated MTPV curve. On the other hand, an online parameter estimation can be combined to ensure the real MTPV operation of the PMSM.

Rated current	i_{max}	280A
DC-link voltage	V_{DC}	280V
Rated speed	$\omega_{m,N}$	1200rpm
Pole pair number	p	4
Stator resistance	R	20mΩ
d-axis inductance	L_{d0}	0.75mH
q-axis inductance	L_{q0}	1.7mH
Flux linkage	Ψ_{F0}	0.14Vs/rad

Table 1: Nominal parameters of the PMSM 1

5 Simulation and experimental results

The simulation model is implemented in Matlab/Simulink to validate the performance of proposed field weakening control scheme. The nominal parameters of the simulated IPMSM are shown in Table 1. The controller is implemented as the a digital controller with sampling frequency 8kHz, while the inverter and the PMSM are simulated as continuous system with smaller execution time. The carrier frequency of the inverter is set to 8kHz. The current and speed are measured by the zero-order-holder at 8kHz. The time constant of the inner current loop is chosen to $\tau = 0.01$s.

The first set of simulations is made to compare the performance of the minimum phase and the proposed overmodulation in the deep field weakening region. The current control is applied to the PMSM and the stator current reference i'_s is set to its rated value. The same current and field weakening controllers are applied to the PMSM for both minimum phase and proposed overmodulation. The simulation results of the minimum phase and the proposed overmodulation are shown in fig. 4 and fig. 5 respectively. For both cases, the mechanical speed of the PMSM ω_m varies from 1000 rpm to 11000 rpm within 0.2 s. From the simulation results in fig. 4, it can be noticed that the PMSM system with the conventional minimum phase overmodulation is no longer stable in the deep field weakening region. However, when with the proposed overmodulation, the PMSM system is still stabilized. The transient current locus in fig. 5 shows that the PMSM is also transiently stable when it enters the generator region.

The second set of simulations is to show the robustness of the proposed field weakening control. A speed control is allied to the PMSM. The simulation results are illustrated in fig. 6 and fig. 7. The speed of the PMSM is controlled to 7000 rpm, which is about 6 times rated speed of the PMSM. The load torque is set to about 80% of the maximum torque at 7000 rpm. Fig. 6 shows the simulations results without parameter mismatch. It can be noticed that transition among the MTPA, constant power and MTPV regions is very smooth. The transient current locus of the PMTM tracks the operating curve and

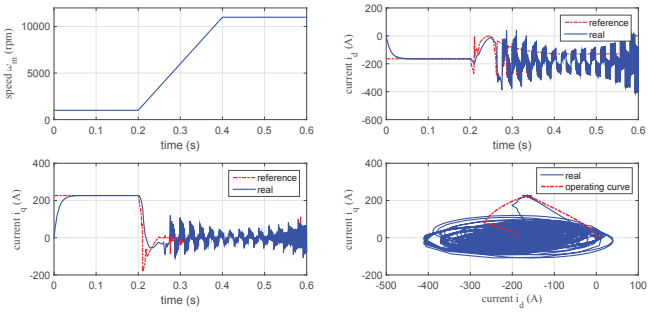

Fig. 4: Simulation results of minimum phase modulation.

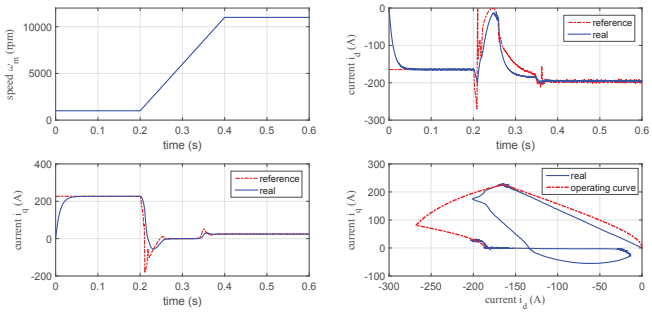

Fig. 5: Simulation results of proposed modulation.

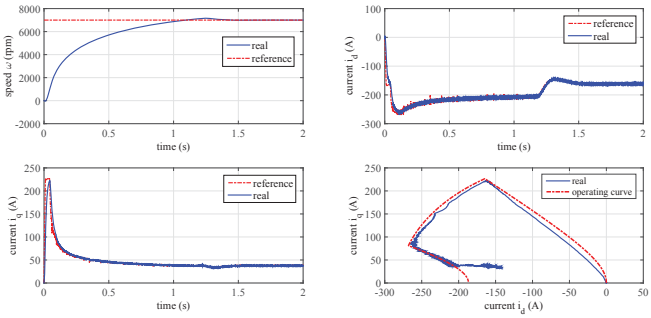

Fig. 6: Simulation results of speed control without parameter mismatch.

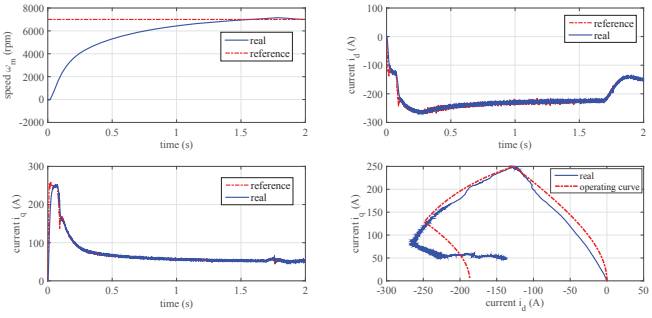

Fig. 7: Simulation results of speed control with q-axis inductance $L_q = \frac{2L_{q0}}{3}$.

converges to the corresponding operating point along the constant voltage ellipse. Fig. 6 shows the simulation results with

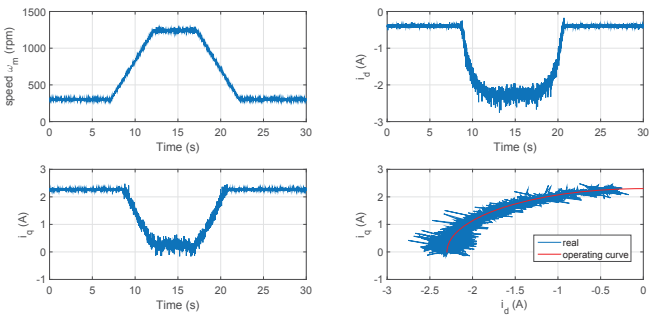

Fig. 8: Experimental results with proposed field weakening control.

Rated current	i_{max}	2.3A
DC-link voltage	V_{DC}	60V
Rated speed	$\omega_{m,N}$	500rpm
Pole pair number	p	4
Stator resistance	R	3.2mΩ
d-axis inductance	L_{d0}	16mH
q-axis inductance	L_{q0}	20mH
Flux linkage	Ψ_{F0}	0.0886Vs/rad

Table 2: Nominal parameters of the PMSM 2

paramter error $L_d = \frac{2L_{q0}}{3}$, which imitates the saturation effect in the PMSM. With parameter error, the transient current locus deviates from the optimum operating curve due to the wrong MTPV curve with displacement on L_q. When compared to the simulation results withaout parameter error, the speed dynamic with L_q error is slowed down due to the deviation from the optimum operating curve. However, the entire system is still stable and the transient current dynamics are still smooths.

The proposed field weakening control algorithm is also validated by the experimental results shown in fig. 2. The experiments are made to another PMSM, whose nominal parameters are shown in table 2. There is no MTPV region for the test PMSM. The speed of the PMSM is drive from 300 to 1250 rpm by the load machine. From fig. 8, it can be noticed that the PMSM is almost with its maximum speed limited by the rated current and DC-link voltage. The current dynamics as well as the current locus show the good performance of the proposed control strategy in the deep field weakening region.

6 Conclusions

In this paper, a robust deep field weakening control is proposed for the PMSM. With the modified overmodulation strategy, the flux of the PMSM is decreasing to fit the voltage constraint during the transient state, which improves the transient stability of the PMSM in the field weakening region. Combining the voltage feedback control and the compensation term of MTPV, a seamless operation of the PMSM can be realized until the deep field weakening range. The simulation and experimental results validate the performance of the proposed control scheme.

References

[1] S. Bolognani, S. Calligaro, and R. Petrella, "Adaptive flux-weakening controller for interior permanent magnet synchronous motor drives," *Emerging and Selected Topics in Power Electronics, IEEE Journal of*, vol. 2, pp. 236–248, June 2014.

[2] M. Tursini, E. Chiricozzi, and R. Petrella, "Feedforward flux-weakening control of surface-mounted permanent-magnet synchronous motors accounting for resistive voltage drop," *Industrial Electronics, IEEE Transactions on*, vol. 57, pp. 440–448, Jan 2010.

[3] C.-T. Pan and S.-M. Sue, "A linear maximum torque per ampere control for ipmsm drives over full-speed range," *Energy Conversion, IEEE Transactions on*, vol. 20, pp. 359–366, June 2005.

[4] B. Cheng and T. Tesch, "Torque feedforward control technique for permanent-magnet synchronous motors," *Industrial Electronics, IEEE Transactions on*, vol. 57, pp. 969–974, March 2010.

[5] S. Kim and J.-K. Seok, "Maximum voltage utilization of ipmsms using modulating voltage scalability for automotive applications," *Power Electronics, IEEE Transactions on*, vol. 28, pp. 5639–5646, Dec 2013.

[6] T.-S. Kwon and S.-K. Sul, "Novel antiwindup of a current regulator of a surface-mounted permanent-magnet motor for flux-weakening control," *Industry Applications, IEEE Transactions on*, vol. 42, pp. 1293–1300, Sept 2006.

[7] Y.-C. Kwon, S. Kim, and S.-K. Sul, "Six-step operation of pmsm with instantaneous current control," *Industry Applications, IEEE Transactions on*, vol. 50, pp. 2614–2625, July 2014.

[8] P.-Y. Lin, W.-T. Lee, S.-W. Chen, J.-C. Hwang, and Y.-S. Lai, "Infinite speed drives control with mtpa and mtpv for interior permanent magnet synchronous motor," in *Industrial Electronics Society, IECON 2014 - 40th Annual Conference of the IEEE*, Oct 2014, pp. 668–674.

[9] H. Liu, Z. Zhu, E. Mohamed, Y. Fu, and X. Qi, "Flux-weakening control of nonsalient pole pmsm having large winding inductance, accounting for resistive voltage drop and inverter nonlinearities," *Power Electronics, IEEE Transactions on*, vol. 27, pp. 942–952, Feb 2012.

[10] S.-M. Sue and C.-T. Pan, "Voltage-constraint-tracking-based field-weakening control of ipm synchronous motor drives," *Industrial Electronics, IEEE Transactions on*, vol. 55, pp. 340–347, Jan 2008.

[11] Z. Lei, X. Shan, W. Xuhui, L. Yaohua, and K. Liang, "A new deep field-weakening strategy of ipm machines based on single current regulator and voltage angle control," in *Energy Conversion Congress and Exposition (ECCE), 2010 IEEE*, Sept 2010, pp. 1144–1149.

[12] Y. Zhang, L. Xu, M. Gueven, S. Chi, and M. Illindala, "Experimental verification of deep field weakening operation of a 50-kw ipm machine by using single current regulator," *Industry Applications, IEEE Transactions on*, vol. 47, pp. 128–133, Jan 2011.

[13] T.-S. Kwon, G.-Y. Choi, M.-S. Kwak, and S.-K. Sul, "Novel flux-weakening control of an ipmsm for quasi-six-step operation," *Industry Applications, IEEE Transactions on*, vol. 44, pp. 1722–1731, Nov 2008.

[14] Y.-C. Kwon, S. Kim, and S.-K. Sul, "Voltage feedback current control scheme for improved transient performance of permanent magnet synchronous machine drives," *Industrial Electronics, IEEE Transactions on*, vol. 59, pp. 3373–3382, Sept 2012.

[15] C. P. G. Franceschini, A. Fratta and A. Vagati, "Control of high performance synchronous reluctance drives," in *in Proc. PCIM 94, Nuremberg, Germany*, 1994, p. 117 126.

[16] S. Lerdudomsak, S. Doki, and S. Okuma, "Voltage limiter calculation method for fast torque response of ipmsm in overmodulation range," in *Industrial Electronics, 2009. IECON '09. 35th Annual Conference of IEEE*, Nov 2009, pp. 1383–1388.

[17] B.-H. Bae and S.-K. Sul, "A novel dynamic overmodulation strategy for fast torque control of high-saliency-ratio ac motor," *Industry Applications, IEEE Transactions on*, vol. 41, pp. 1013–1019, July 2005.

[18] J.-K. Seok, J.-S. Kim, and S.-K. Sul, "Overmodulation strategy for high-performance torque control," *Power Electronics, IEEE Transactions on*, vol. 13, pp. 786–792, July 1998.

[19] M. Preindl and S. Bolognani, "Model predictive direct torque control with finite control set for pmsm drive systems, part 2: Field weakening operation," *Industrial Informatics, IEEE Transactions on*, vol. 9, pp. 648–657, May 2013.